INVESTIGATION OF CREEP
BY USE OF CLOSED LOOP
SERVO-HYDRAULIC TEST SYSTEM

by

Han C. Wu and J. C. Yao

Report G302-81-001

Prepared for
NASA-Langley Research Center
Grant No. NSG 1499

Division of Materials Engineering
The University of Iowa
Iowa City, Iowa 52242

November 20, 1981

ABSTRACT

Creep tests have been conducted by means of a closed loop servo-controlled materials test system. These tests are different from the conventional creep tests in that the strain history prior to creep may be carefully monitored. Tests have been performed for aluminum alloy 6061-0 at 150°C and have been monitored by a PDP 11/04 minicomputer at a preset constant plastic-strain rate prehistory. The results show that the plastic-strain rate prior to creep plays a significant role in creep behavior.

The endochronic theory of viscoplasticity has been applied to describe the observed creep curves. The concepts of intrinsic time and strain rate sensitivity function are employed and modified according to the present observation.

CHAPTER I

INTRODUCTION

The governing equations of the creep behavior for metals attract much of the current research interest. This interest was stimulated by the increasingly stringent demands that are being made by modern technology for the efficient performance of metallic structure. In addition, recent developments in material testing techniques show that the classical idealization of real material behavior is no longer adequate.

Historically, Andrade [1] was among the first to describe three stages of creep [primary (transient), secondary (steady) and tertiary creep], and developed special equipment to perform creep tests under constant stress rather than constant load. Materials for technological application, where creep was an important factor, were being developed rapidly in the 1920's. This lead to the writting of the first book [2] on the creep behavior of technological materials (steels) by Norton in 1929. In that book Norton related the creep rate to stress by a power law, i.e. $\dot{\epsilon} \propto \sigma^n$. The background of knowledge

developed in plastic flow at high temperature up to 1950's allowed for rapid development in this field in the ensuing years. During the last 30 years, a large volume of books such as Garofalo [3], Rabotnov [4], Gittus [5], and Conway [6] and numerous research articles were published on this subject.

However, there still exists an unresolved problem related to the role played by strain hardening during creep. This problem is important in the investigation of creep subject to variable stress. Although the conventional time-hardening or strain-hardening (or their combination) models have been employed to discuss this effect, this approach is valid only for the description of creep and may not be applicable to describing stress variation arising from other loading histories. At the service load, it is likely that several types of loading histories may be present (possibly including creep and cyclic loading, etc.) either simultaneously or in sequence. The description of this complex behavior calls for a unified approach. Fortunately, recent progress in the understatnding of the strain-rate and strain-rate history effect has suggested that non-elastic deformation of metals is basically rate-dependent plastic behavior, which gives hope for developing a new approach to account for strain hardening during creep. In this aspect the work of Rice [7], Hart [8], Miller [9], Valanis and Wu

[10], Wu and Yip [11] and Cernocky and Krempl [12] should be mentioned. These investigations have been aimed to provide a general representation of plastic behavior of metallic materials. The classical theories have been known to be in need of improvement.

In this report, creep is viewed as a special case of the general mechanical behavior of material. The response function for creep is deduced from the general constitutive equation of the material under study by imposing the condition of constant stress. This viewpoint is shared by such research workers as Valanis and Lalwani [13] and Wu and Chen [14].

In this investigation, creep tests were conducted by use of a MTS materials test system. This is different from a conventional creep test in that the strain history prior to creep may be carefully controlled. Several sets of test were performed for Aluminum alloy 6061-0 at 150°C (300°F). A PDP 11/04 minicomputer was employed to control the tests. All tests were conducted with a constant plastic-strain rate prehistroy. The results show that plastic-strain rate prior to creep plays a significant role in creep behavior of metals. The Endochronic Theory of Viscoplasticity which was originally developed by Valanis [15,16,17] is applied to describe the observed creep curves. The concepts of intrinsic time and strain rate sensitivity function are employed and modified according to the current observations.

CHAPTER II

EXPERIMENTS

Material and Specimens

The material used in this investigation was a 6061-T6 Aluminum alloy. Specimens were machined from 2.54cm×0.476cm (1"×3/16") rectangular bars. Figure 1 shows the geometry of the specimens.

The machined specimens were cleaned to remove the distorted surface layer resulted from machining, then wrapped in aluminum foils and annealed at 343°C (650°F). They were heated for 150 minutes and then oven cooled for one day.

Considering the system capabilities and the material properties, three conveniert plastic-strain rates: 10^{-3}, 10^{-4} and 10^{-5} S^{-1}; and three creep stress levels: 75.8, 82.7 and 89.6 MPa (i.e. 11, 12 and 13 ksi) were chosen for this investigation. Also, 150°C (300°F) was chosen as the test temperature and all creep tests were terminated after 90 minutes of creep. The specifications of the specimens were shown in Table 1.

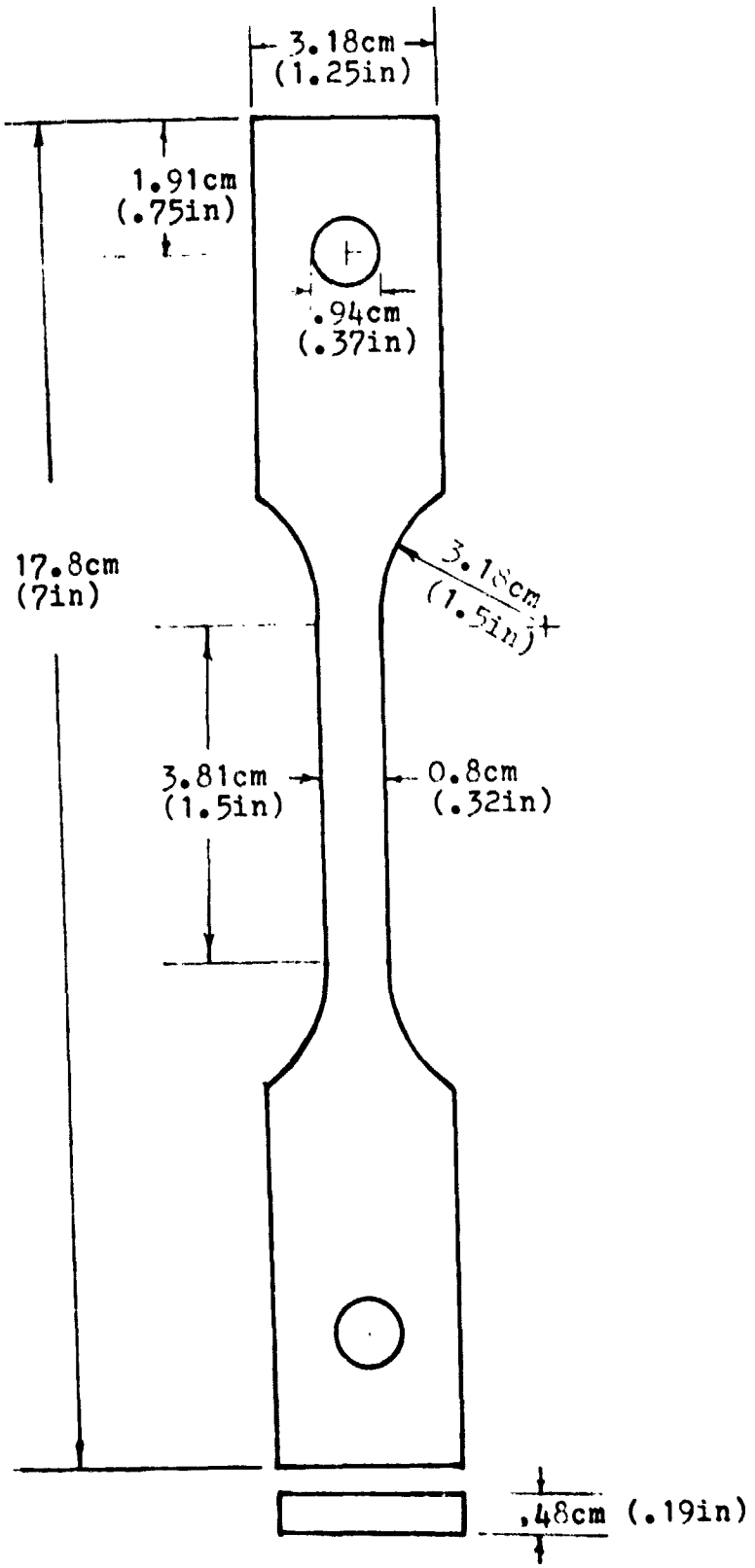

Figure 1: Specimen Geometry

Table 1

Specimen Specification

Specimen Number	Prehistory Strain-rate (s^{-1})	Creep Stress (MPa)	Specimen Area (cm×cm)	Elastic Modulus (MPa)
A11	10^{-3}	75.8	0.41077	56001.
A13	10^{-3}	89.6	0.40561	65571.
B11	10^{-4}	75.8	0.40644	62786.
B12	10^{-4}	82.7	0.40529	57849.
B13	10^{-4}	89.6	0.39702	58794.
C11	10^{-5}	75.8	0.40097	67895.
C13	10^{-5}	89.6	0.39181	66516.

Apparatus

A closed loop, hydraulic driven, servocontrolled test system (MTS system) was used for all tests. This test system was operated as a normal closed loop system but derived its command signal from a minicomputer. The essential elements of the test system are depicted schematically in Figure 2 and can be described as two distinct subsystems, one being analog and the other digital.

Analog hardware

The analog hardware of the system consists of a load frame, a hydraulic power supply and an analog electronics controller. The load frame assembly consists of a two-column frame, a servo hydraulic actuator, and a load cell mounted on the top crosshead. Hydraulic power required to operate the system is supplied by a 37.9 lpm pump, which is located in the annex pump room to provide noise isolation. The analog electronics includes the servo controller, transducer conditioners, and the feedback selector.

Digital hardware

The digital subsystem consists of a computer processor, its input/output peripherals, and the modules necessary for interfacing the analog and digital components of the whole system. The central processor is a PDP 11/04 minicomputer with 32K words of memory. A double/single density diskette unit is used for mass storage.

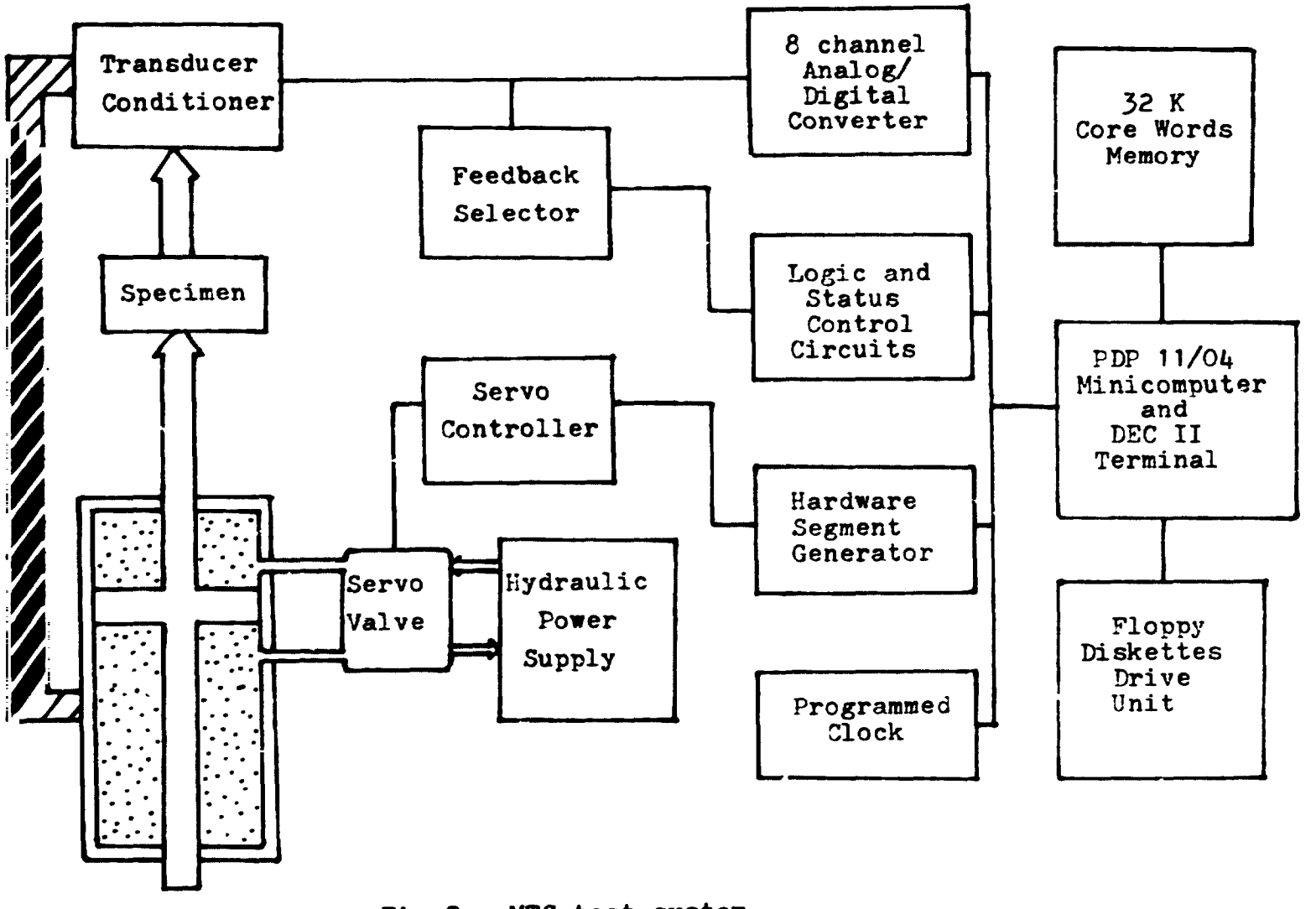

Fig 2: MTS test system

Since the minicomputer cannot communicate directly with the analog servo hydraulic system, an interface between the computer and the servo system is necessary. This includes a programmable clock that interrupts the computer and drives the real time software, allowing analog input/output to proceed on a real time basis. The clock is programmable in that it allows the system operator, through software command, to set the clock rate that best suits the test process.

Logical and status control interrupt circuits are also included in the interface. They allow the computer to change the control feedback signal with the servo hydraulics in operation, and permit the break-keys to be used for real time and programmed software interrupts. Also included in the interface is a digitally controlled analog output device called a Hardware Segment Generator (HSG). This device is capable of producing either ramp or haversine waveforms. An eight channel continuous reading analog-to-digital converter is used for data acquisition. Each data channel is automatically updated at maximum converter rates thereby increasing the sampling speed and reducing the time skew in acquiring data.

System software

BASIC which is a high level, interactive computer language is employed. Thus, the operator needs no knowledge of computer machine language in order to develop and run programs for material testing. Assembly language subroutines which are included in the system software permit real time , high speed function generation, and data acquisition.

Analog command functions, utilizing the HSG, are defined by an external function subroutine. This subroutine, which is called by typing "FG1", is capable of the following:

1. sine, block or random waveform;
2. constant or varying frequencies;
3. ramp or haversine segments.

The assembly language subroutine, "DACQ", utilizes the continuously reading analog-to-digital converters for data acquisition. The external function has operating modes described as follows:

1. immediate single return (reading) from a single channel;
2. peak/valley detection and maximum/minimum detection;
3. continuous samples with constant time intervals;
4. discrete readings upon the occurrence of an auxiliary event;

5. time since the last peak or event.

As data are acquired using this external function, they are saved in arrays thereby permitting on-line data analyses as a test is in progess. Other available subroutine functions include automatic switching of the feedback control signal (MSW1) and the use of keyboard intersrupt registers (BUTN) that allows an interrupt to a user written subroutine.

Testing Procedure

Preparation of loading paths

As mentioned in the Introduction, the material behavior is strongly affected by plastic-strain-rate and its history. For the purpose of simplicity all creep tests were conducted with a constant plastic-strain-rate preloading. A preset loading path was needed for testing requirement since the test system can only control the total-strain rate and not the plastic-strain rate.

For each chosen plastic-strain-rate, the loading path was determined from an equivalent total-strain-rate controlled simple tensile test. This was done by using a computer interpolation program to calculate the suitable ε-t data and storing these data in a data file for later use.

Execution of Pre-programmed test

A BASIC computer program was written for the test in which the plastic-strain-rate was kept constant during the loading stage and the stress was kept constant after the stress reached the preset creep stress. This operation involved a mode switching at the beginning of the creep stage.

Computing the Elastic Modulus

Before the above program was executed, the specimen was mounted to the grips under the stroke controlled mode and then the furnace cabinet was heated up to 150°C (300°F). At the beginning of the program, the system requested the operator to enter all necessary control data for the test. After all of the data had been entered and verified as correct, the system then switched the control mode from stroke to load and increased the stress to half of the approximate yield-stress in order to calculate the elastic modulus. The elastic modulus was determined by least square fitting method from data acquired by the "DACQ" subroutine. After the modulus had been calculated the system then unloaded the specimen to zero stress and waited for the next instruction.

Constant plastic-stran-rate loading

Since the elastic modulus had been determined and the control signal had also been reduced to zero, the system then switched the control mode from load to strain. By using the Hardware Segment Generator and the determined ε-t data, the specimen was pulled according to a constant plastic strain rate path. In the mean time, the data acquisition routine (DACQ) kept acquiring the stress and strain data and storing these data in the output data file. During the loading stage, the computer kept monitoring the stress magnitude (about 200 data/sec). As soon as the stress signal reached the pre-set creep stress, the computer switched the system to load control mode and then kept the stress at this constant magnitude.

Creep Test

During this stage the load was kept constant and the creep data was acquired in every appropriate time interval. In order to observe the initial creep strain rate, the creep data were acquired every 2 seconds during the first 2 minutes. But, as the creep time ellapsed the time interval was increased to 120 seconds. For the purpose of accuracy, every data was acquired several times at the beginning of each time interval, and the mean value of these acquired data were calculated to minimize the error caused by machine noise.

As the time reached the pre-set limit, the computer then decreased the loading to zero and printed the experimental result on the terminal.

CHAPTER III

CREEP THEORY OF ALUMINUM 6061-O

In this investigation, the endochronic theory of viscoplasticity is applied to tackle the problems associated with creep. A brief summary of this theory is given in Appendix A. New developments have been made in this chapter according to the current observations.

The intrinsic time scale function

From equation (A7), the intrinsic time scale function was originally defined as

$$d\zeta/dz = 1 + \beta\zeta \tag{1}$$

It was observed by Wu and Yip [11] that this z-ζ relation was reasonable for monotonic and "simple" loading types. For more complex loading, such as cyclic loading, this equation would lead to difficulties. Specifically, a steady state cannot be achieved. For a more reasonable representation, the following relationship for ζ and z is considered by Wu and Yip [11]:

$$d\zeta/dz = C - (C-1)e^{-\beta_2 z} \tag{2}$$

which may be integrated to yield:

$$\zeta = C\,z + \frac{C-1}{\beta_2}\,(e^{-\beta_2 z}-1) \tag{3}$$

where C and β_2 are material parameters. It should be mentioned that for the infinitesimal strain range, equation (2) has been shown in [13] to reduce to equation (1).

The strain rate sensitivity function

The strain rate sensitivity function introduced in equation (A8) is generally a function of the plastic strain θ and the strain rate $\dot{\theta}$, i.e. $k=k(\theta,\dot{\theta})$. In the k-θ-$\dot{\theta}$ space, the shape of the surface is determined by the material itself, it may vary with the range of strain rate. It was discussed by Wu [14] that during the constant plastic-strain-rate loading stage, the stress-strain curve is determined by specifying any two of the three quantities σ, θ and $\dot{\theta}$. Therefore, for the creep stage of the constant strain-rate preloading creep test, only two of the three quantities are independent, i.e. the creep stress σ^*, the initial creep strain θ_s and the plastic strain rate $\dot{\theta}$. The strain-rate sensitivity function during the process of creep is represented by

$$k(\theta,\dot{\theta}) = k(\sigma^*,\theta_s,\dot{\theta}) \tag{4}$$

One form of the strain-rate sensitivity function was assumed in [11] from the experimental constant-strain-rate stress-strain curve as

$$k(\dot{\theta}) = 1 - \beta_1 \ln\left(\frac{\dot{\theta}}{\dot{\theta}_0}\right) \tag{5}$$

where β_2 is a material constant and $\dot{\theta}_R$ is a reference strain rate.

This linear form of function $k(\dot{\theta})$ in the semi-log plot fits the data nicely for annealed commercially pure aluminum in the strain rate range of 10^{-4} - 10^{3} S^{-1}, and mild steel at constant strain-rate in the range of 10^{-4} - 10^{1} S^{-1}. However, in the current investigation, it was found that the k function was not a straight line for annealed 6061 aluminum alloy in the strain range of 10^{-6} - 10^{-3} S^{-1}. In order to find a suitable strain rate sensitivity function k, it was observed that the changing rate of k value was decreasing with the increasing strain-rate (in logarithmic coordinate). Similarly, the trend also indicates that the changing rate of k value will decrease as the strain-rate declines to steady state. With this thought in mind, the following equation is proposed:

$$k(\sigma^*, \theta_s, \dot{\theta}) = 1-\beta_c(\sigma^*, \theta_s)\text{ARCSINH}(\beta_2 \ln(\frac{\dot{\theta}}{\dot{\theta}_R})) \qquad (6)$$

where β_2 is a material constant and β_c is a function of σ^* and θ_s. This equation has been used in the present investigation and the result obtained is quite encouraging.

Governing equation of the Creep curve

The constitutive equation (A5) and the new definition of intrinsic time given by (A7) and (2) are now applied to describe the creep phenomenon.

In the present representation it is assumed that a creep test consists of two stages. The first stage is a tensile testing at constant plastic-strain-rate θ_0, during this stage the intrinsic time scale increases from zero to z_0, and the intrinsic time relation is defined as $d\zeta/dz=1+\beta\zeta$. For simplicity, during this stage, the strain-rate sensitivity function is assumed to be a function of strain-rate only, i.e. $k=k(\theta)$.

The second stage is the creep stage where the stress is kept constant, during this stage the intrinsic time increases from z_0 to z as creep strain developes, and the intrinsic time scale relation is defined as

$$\frac{d\zeta}{dz} = e^{\beta z_0}[C - (C-1)e^{-\beta_1(z-z_0)}] \qquad (7)$$

Thus, when $z=z_0$, the relation $d\zeta/dz=1+\beta\zeta$ is recovered.

Equation (A5) becomes

$$\sigma^* = \frac{E_0}{a_0}\int_0^z \delta(z-z')\frac{d\theta}{dz'}dz' + \int_0^z E_0 e^{-\alpha(z-z')}\frac{d\theta}{dz'}dz' + \int_{z_0}^z E_0 e^{-\alpha(z-z')}\frac{d\theta}{dz'}dz' \qquad (8)$$

This equation may be simplified to yield

$$\sigma^* = I(z) + R(z) + \sigma_y^0 \frac{d\theta}{dz} \tag{9}$$

with

$$I(z) = C_1 e^{-\alpha z} \tag{10}$$

and

$$R(z) = -e^{-Az}\{C_1[e^{(A-\alpha)z} - e^{(A-\alpha)z_0}] - \frac{C}{A}(e^{Az} - e^{Az_0})\} \tag{11}$$

where

$$C_1 = \frac{1}{k_0}\left(\frac{E_1}{\alpha+\beta}\right)\{e^{(\alpha+\beta)z} - 1\} \tag{12}$$

$$A = E_1/\sigma_y^0 + 1 \tag{13}$$

$$C_2 = E_1\sigma^*/\sigma_y^0 \tag{14}$$

During the creep process, equations (A8), (7) and (9) combined to yield

$$k(\theta,\dot{\theta}) = \sigma_y^0 h(z)/(\sigma^* - R(z) - I(z)) \tag{15}$$

here h(z) is defined as

$$h(z) = e^{\beta z_0}[C - (C-1)e^{-\beta(z-z_0)}] \tag{16}$$

Hence, given a function $k(\theta,\dot{\theta})$, equation (15) can lead to the determination of a creep curve. But, equation (15) is not a suitable function for developing a computer program for creep calculation. An explicit form of the θ-t relationship is needed for computer programming.

Explicit form of θ-t function

From equation (9), let $g(\sigma^*, z)$ be defined as

$$g(\sigma^*, z) = \frac{d\theta}{dz} = \frac{1}{\sigma_y^*}[\sigma^* - I(z) - R(z)] \tag{17}$$

it is obtained from equations (6), (15) and (17) that

$$\beta_2(\ln\frac{\dot{\theta}}{\theta_R}) = \text{SINH}\,[\frac{1}{\beta_c}(1 - \frac{h(z)}{g(\sigma^*, z)}] \tag{18}$$

By introducing

$$\dot{\theta} = \frac{d\theta}{dt} = \frac{d\theta}{dz}\frac{dz}{dt} \tag{19}$$

Equation (19) leads to

$$\int_{z_o}^{z} g(\sigma^*, z)e^{-\frac{1}{\beta_2}\text{SINH}[\frac{1}{\beta_c}(1 - \frac{h(z)}{g(\sigma^*, z)}]}dz' = \int_0^t \dot{\theta}_R\,dt \tag{20}$$

which is a z-t relation.

Also, from equation (9)

$$[\sigma^* - I(z) - R(z)]dz = \sigma_y^* d\theta \tag{21}$$

Integration of this equation gives

$$\theta = \theta_o + \frac{1}{\sigma_y^*}[\sigma^*(1 - \frac{E_1}{\sigma_y^* A})(z - z_o) + \frac{e^{Az}}{A}(ce^{-\alpha z_o} - \frac{C}{A})(e^{-Az} - e^{-Az_o})] \tag{22}$$

Since both the z-t and θ-z relationships were known, a computer program was developed for calculating the creep curve. This computer program, utilizing the IMSL-ZXSSQ function minimization subroutine, was used for finding the material constants of Aluminum alloy 6061-0.

CHAPTER IV

RESULTS AND DISCUSSION

Experimental results

Since the experiments were conducted by the PDP 11/04 minicomputer and the experimental data were stored in floppy diskettes, it would not take much effort to repossess the data for further analysis.

The loading path of specimen #B12, shown in Figure 3 , shows that the plastic-strain-rate was successfully controlled. From this investigation, both plastic-strain-rate and strain-rate history exhibit noticeable effect on the subsequent behavior of Aluminum alloy 6061-0. The material constants of 6061-0 Al, calculated by using the governing equations (20) and (22), are listed in Table 2.

The theoretical and experimental results are shown in Figures 4-11. The results show that reasonably good agreement has been achieved by use of the constants listed.

Plastic-strain-rate effect during loading

The plastic-strain-rate effect during loading is now discussed in terms of the material response of 6061-0 aluminum alloy. Figure 4 shows the stress-strain curves of

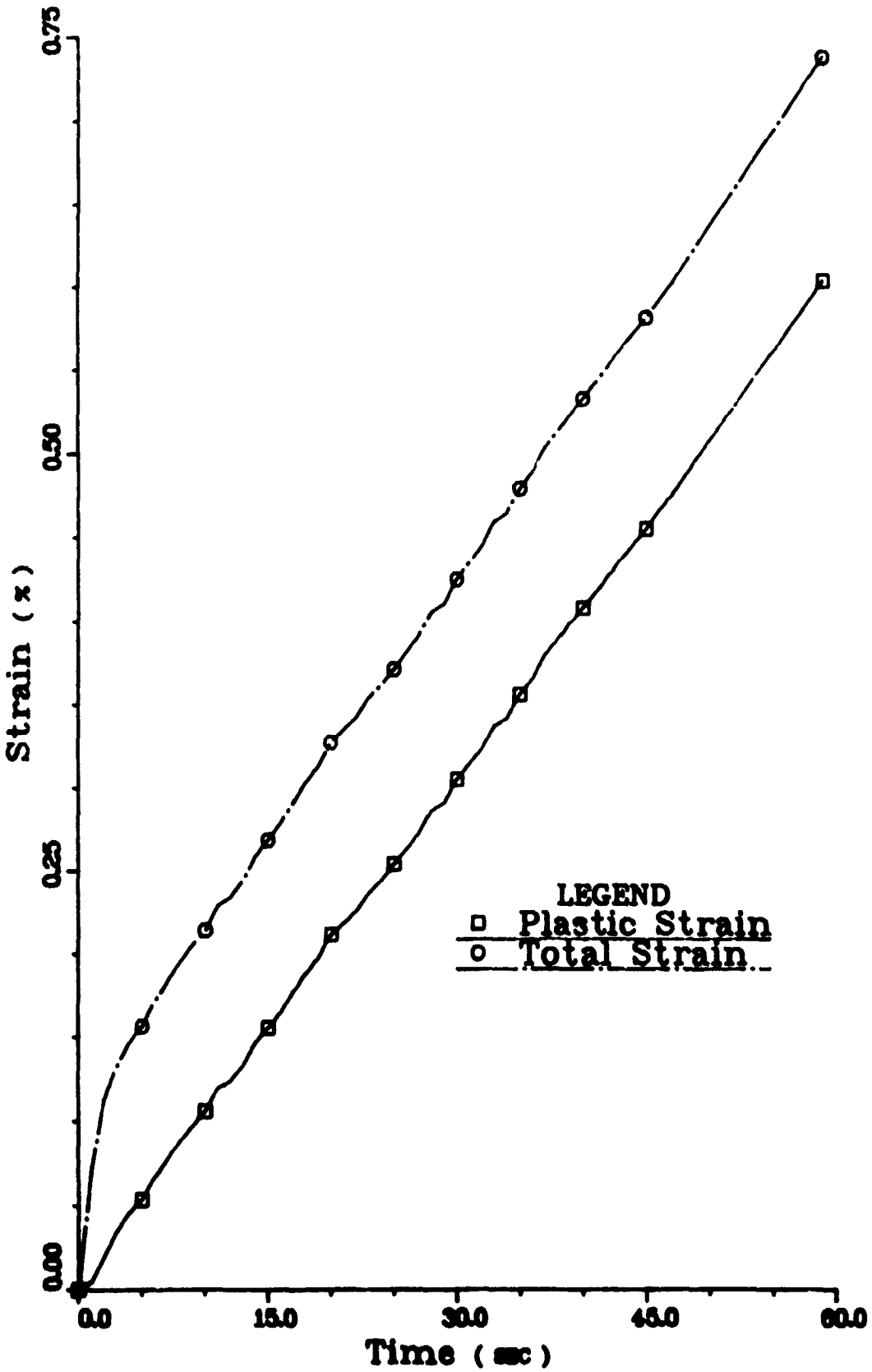

Fig 3: Strain–Time Profile

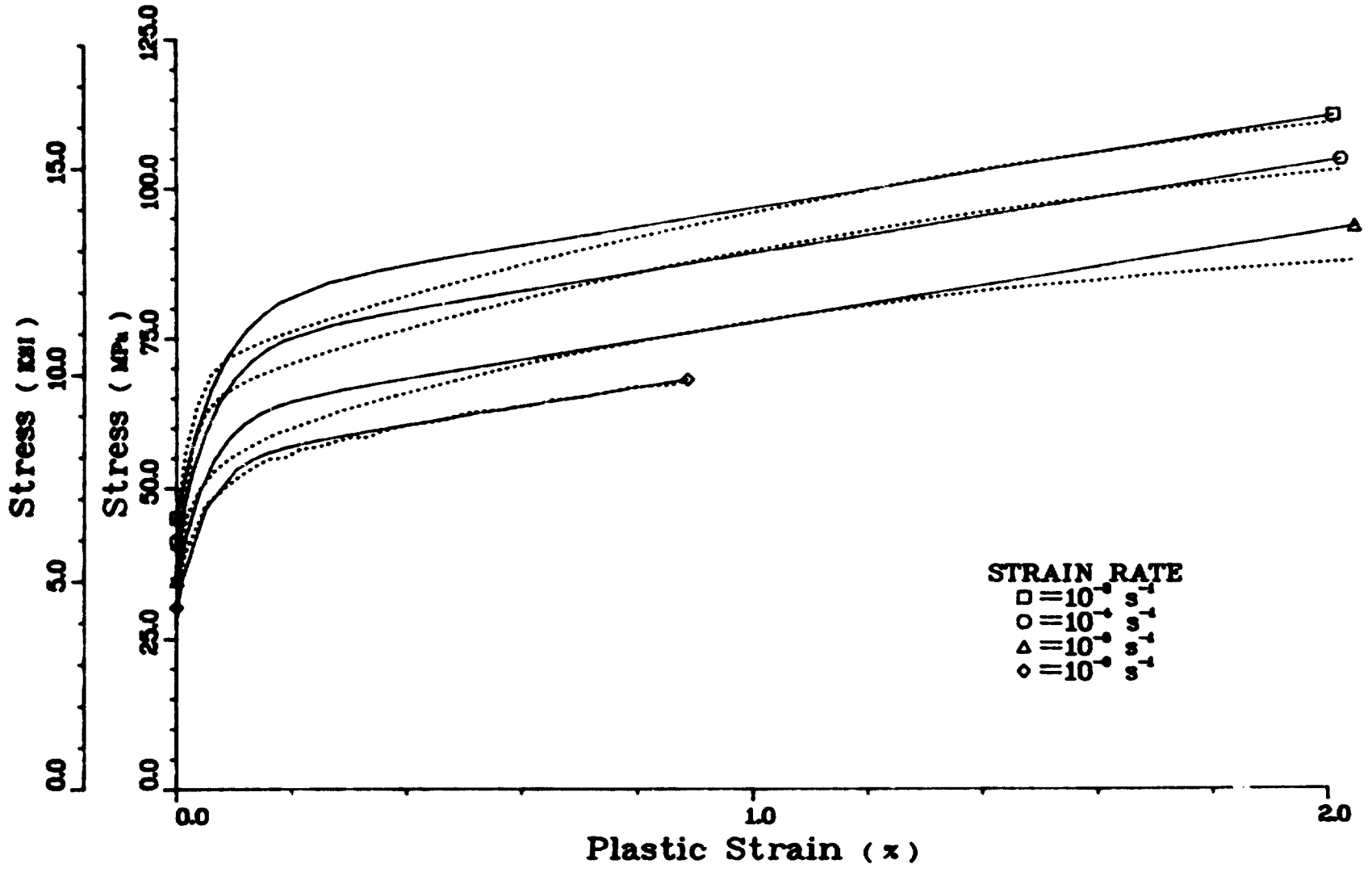

Fig 4: Constant Strain-Rate Stress-Strain Curves

Table 2

Material Parameters

$\alpha = 1850.$	$\beta = 25.$
$\beta_1 = 9500.$	$\beta_2 = 0.6914$
$C = 2.4$	$E_1 = 2.1\times10^3$ ksi (14.5×10^3 MPa)
$\sigma_y^0 = 5.$ ksi (35.4 MPa)	

the loading stage for respective strain rates and an additional loading curve of 10^{-6} s^{-1} is added for comparison. In the figure, dotted curves denote experimental data and solid curves denote theoretical results. As predicted, these four curves are almost parallel to each other and, the higher strain-rate has the stiffer response.

But, it is also noticed that the curve of 10^{-4} is closer to the curve of 10^{-3} rather than the curve of 10^{-5}. This phenomenon, as mentioned in an earlier section, makes obsolete the linear form of the strain-rate sensitivity function and requires a nonlinear form given by equation (6). The curve of strain-rate sensitivity function versus logarithmic strain-rate is shown in Figure 5. It should be pointed out that owing to the nature of this function, the reference strain rate should be located at the point of

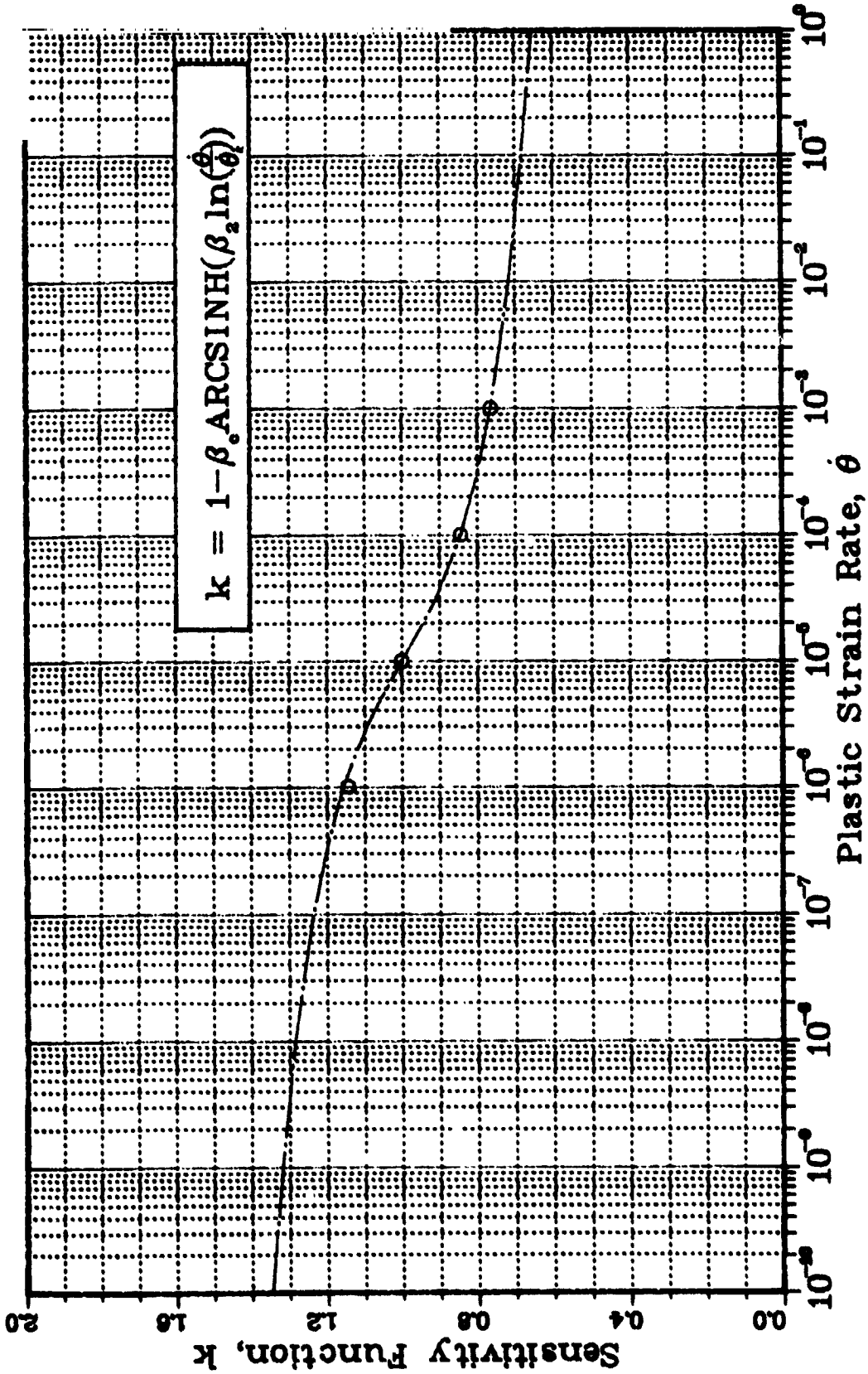

Fig 5: Strain–Rate Sensitivity Function

inflection. The experimental data show that the reference strain-rate is around 10^{-5} s^{-1}. For calculational convenience, 10^{-5} s^{-1} was chosen as the reference strain rate.

Strain-rate history effect

The experimental creep curves of different strain-rates at loading, with the same stress level, are shown in Figure 6 and Figure 7. Also shown in Figure 8 are creep curves during the first 120 seconds of Figure 6.

An interesting phenomenon was observed in these figures. Although the accumulated creep strain of the specimen with higher strain-rate loading history, e.g. #B11, is smaller than that of the specimen with lower strain-rate prehistiry, e.g. #C11, the initial creep-strain-rate of the former is still greater than that of the latter. But, because of the higher magnitude of the initial plastic strain, the creep-strain-rate of #C11 soon exceeds that of #B11, as does the accumulated creep-strain.

Theoretical results

The theoretical creep curves, calculated by using equations (20) and (22), are shown in Figures 9, 10 and 11, in which the dotted curves are experimental and the solid curves are theoretical. The results show that reasonable agreement has been obtained, especially for the tests of 10^{-4} s^{-1} plastic-strain-rate.

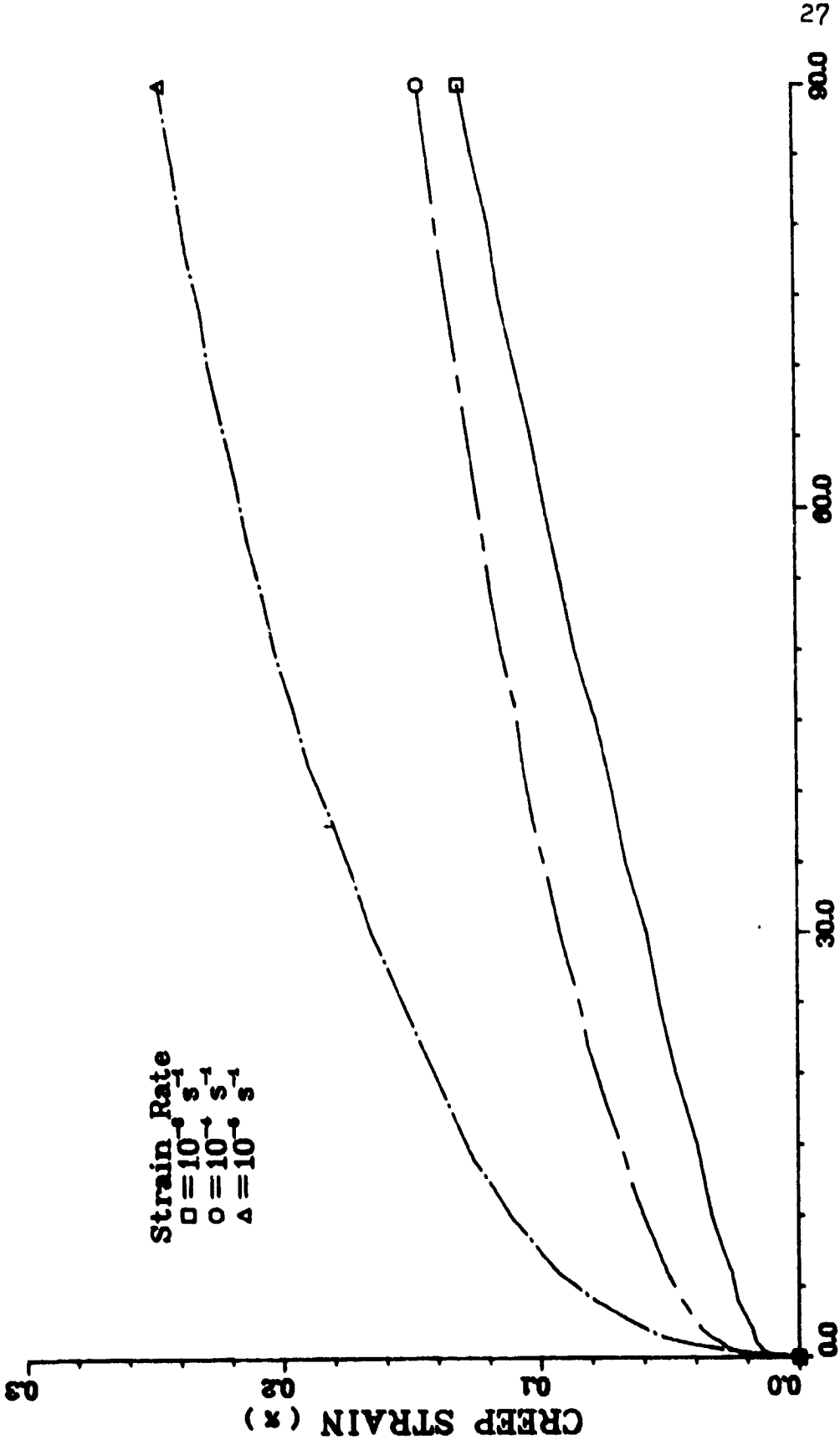

Fig 6: Experimental Creep Curves (75.8 MPa)

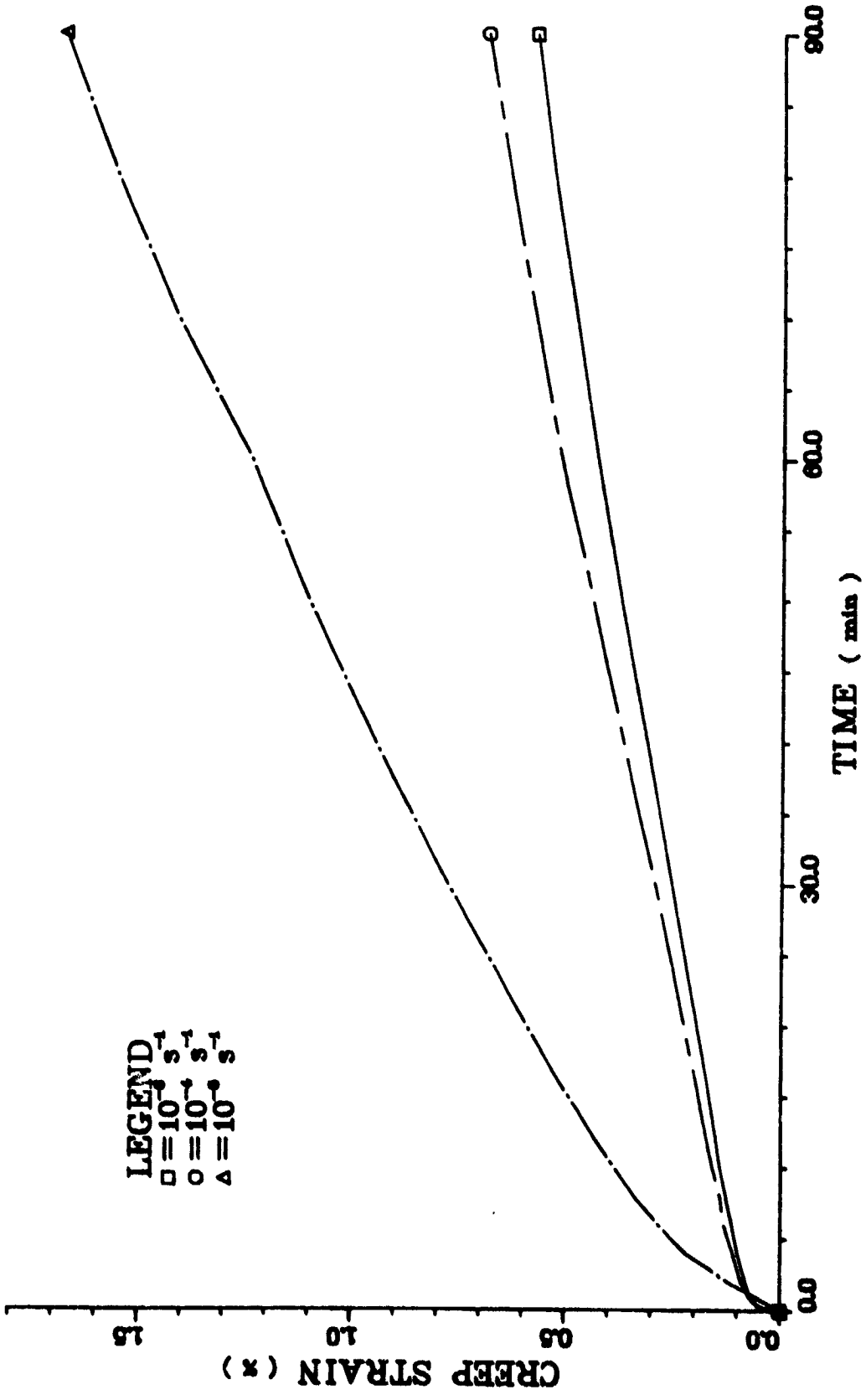

Fig 7: Experimental Creep Curves (89.6 MPa)

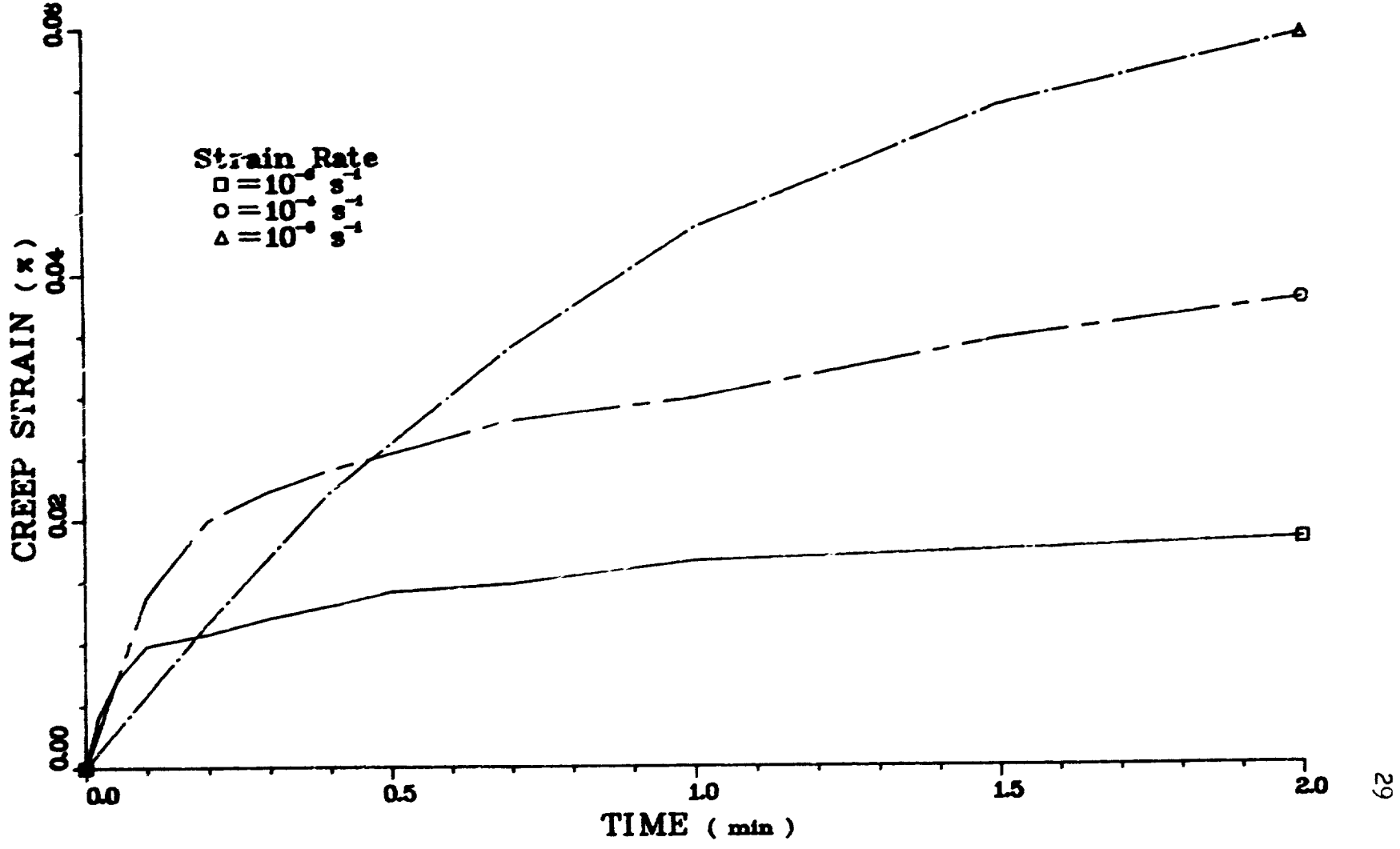

Fig 8: Initial Creep Curves (75.8 MPa, First 120 sec)

As mentioned in the last section, the initial plastic strain also affect the accumulation of the creep-strain. Recalling from equation (6), the function $\beta_c(\sigma^*,\theta_0)$ has been introduced as a function of creep-stress σ^* and initial plastic-strain θ_0. For finding the form of the β_c function, an exponential expression was proposed as follows:

$$\beta_c = (a_1+a_2e^{a_3\sigma^*})(a_4+a_5e^{a_6\theta_0}) \tag{23}$$

From experimental data, the coefficients of equation (23) was determined as follows:

a_1 =-1.3394 a_4 = 0.07182

a_2 = 9.6271 a_5 = 0.05136

a_3 =-0.1139 a_6 = 1.62705

The theoretical and experimental β_c values are given in Table 3. The result shows that this exponential form is suitable for the β_c function for the strain rate range considered. However, for further verification, more experimental data are needed indeed.

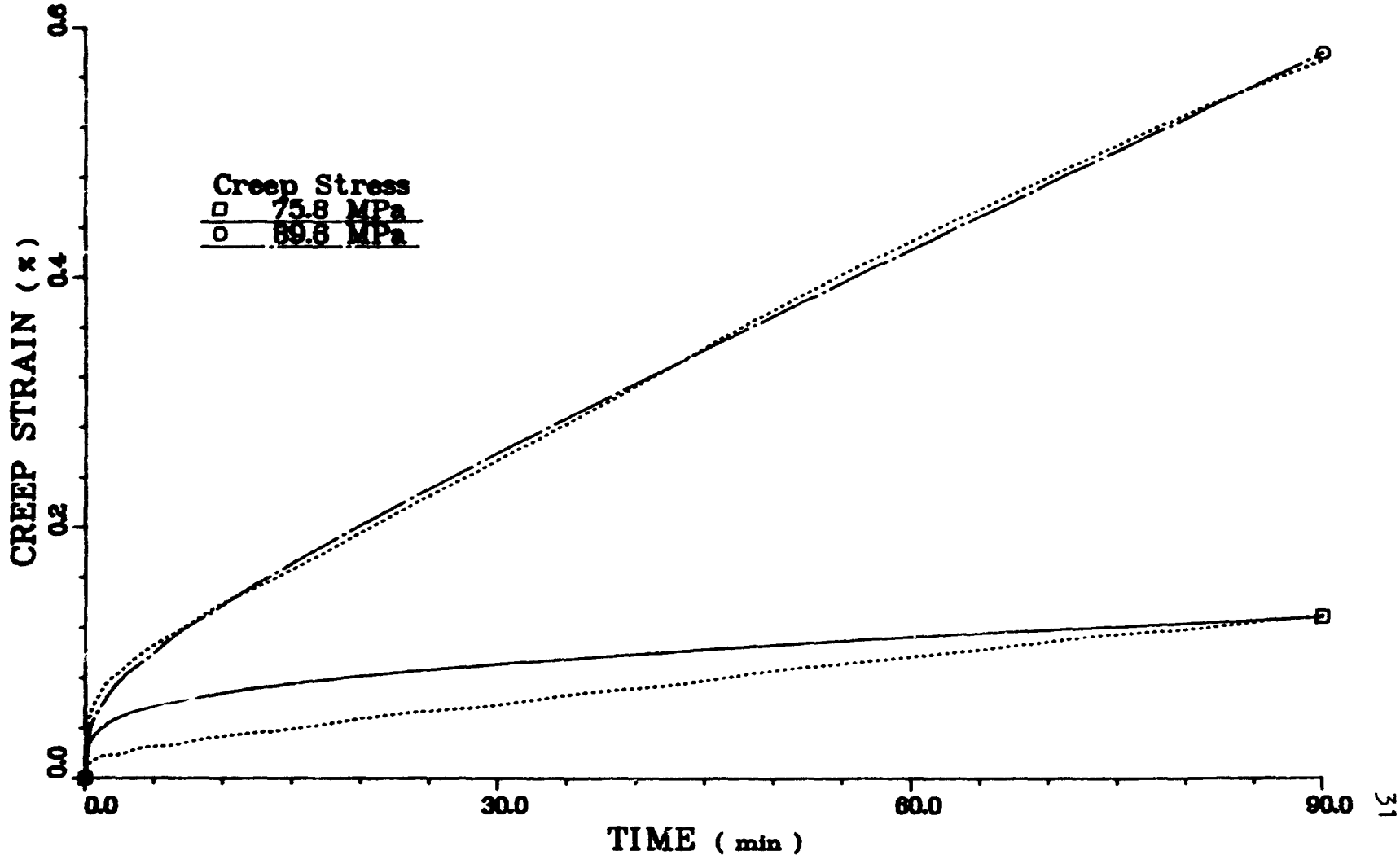

Fig 9: Theoretical Creep Curves (10^{-3} s^{-1})

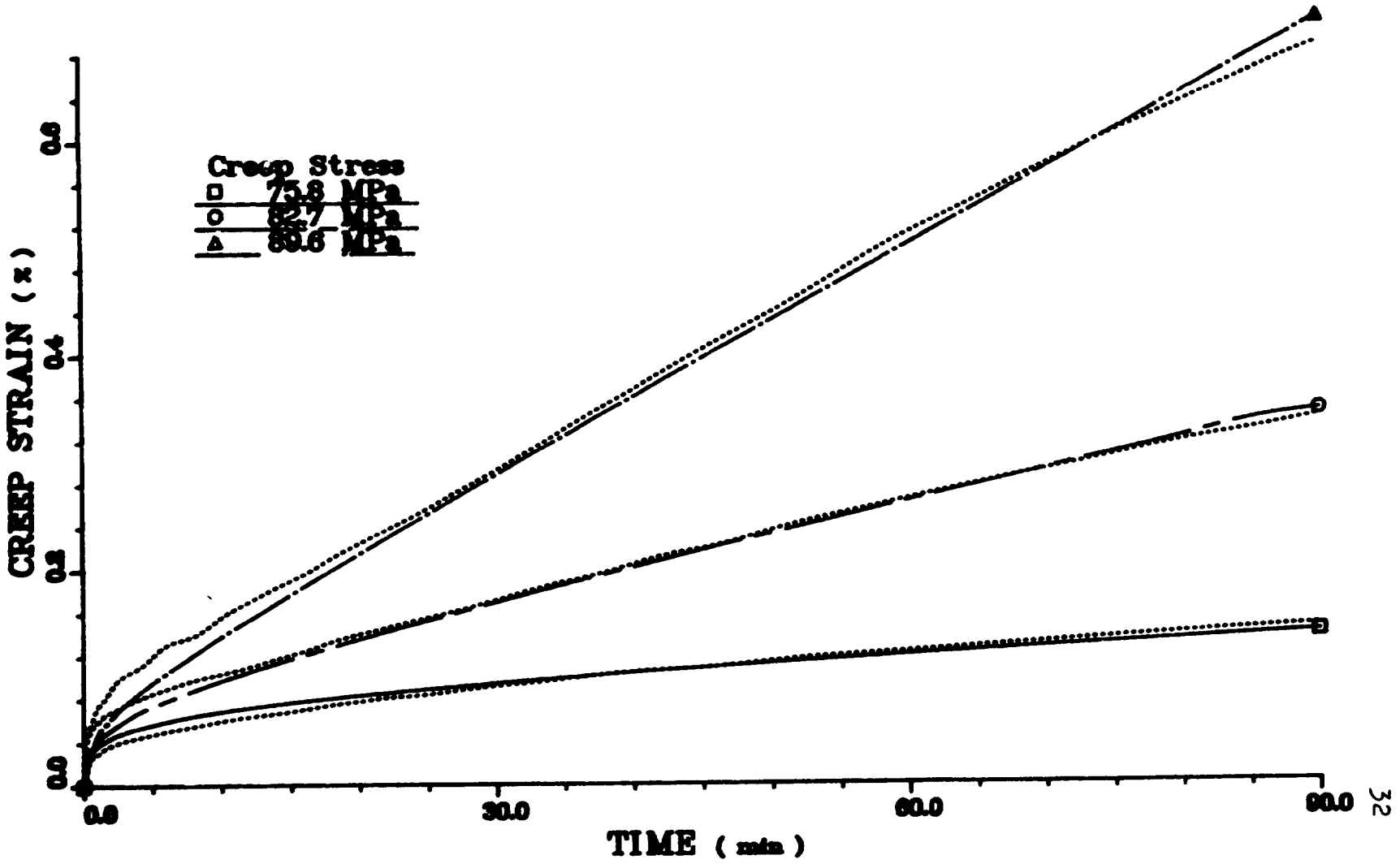

Fig 10: Theoretical Creep Curves (10^{-4} s^{-1})

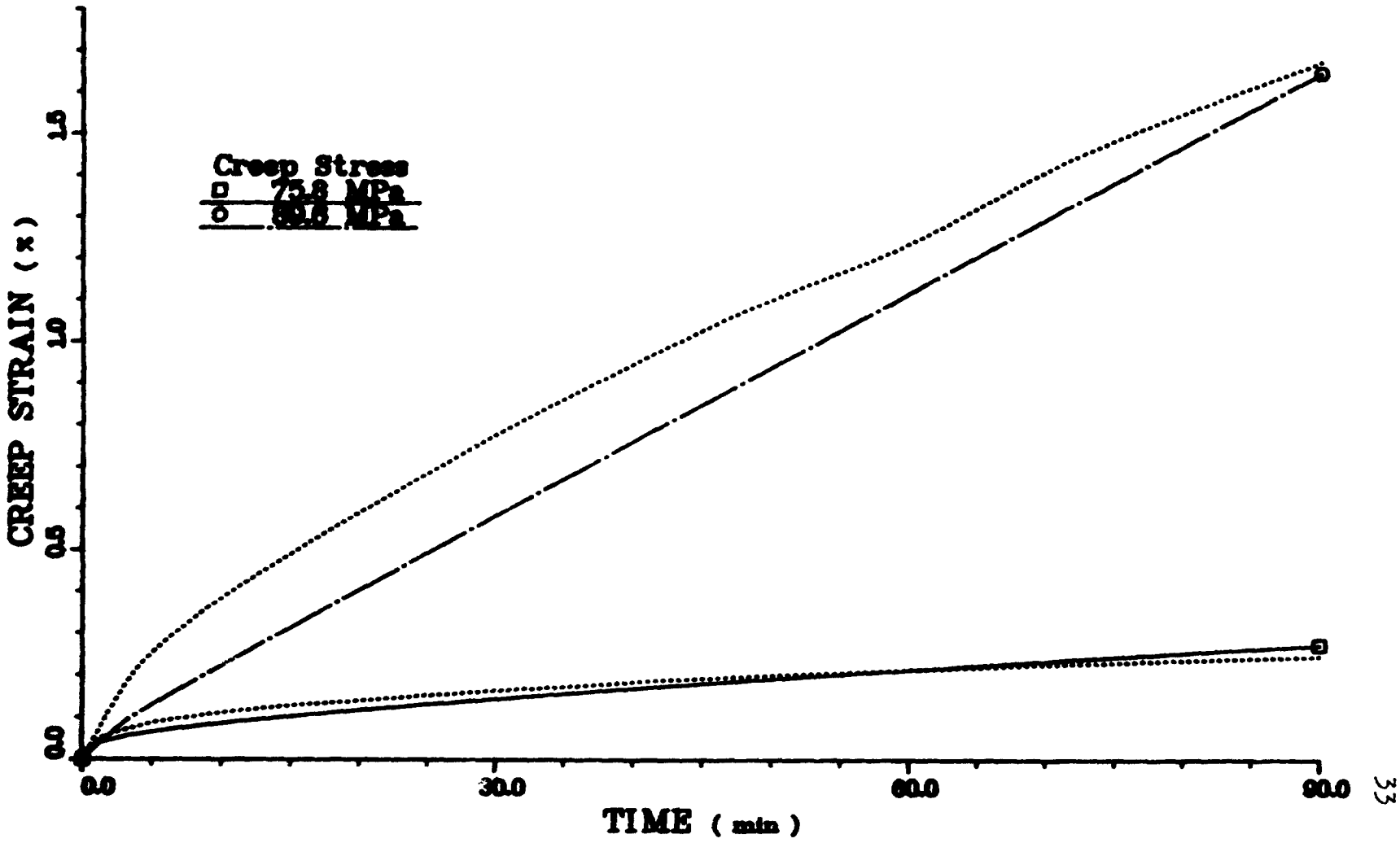

Fig 11: Theoretical Creep Curves (10^{-6} s^{-1})

Table 3

The values of β_c

Specimen Number	Creep Stress (MPa)	Initial Strain (%)	β_c (Exper.)	β_c (Theory)
A11	75.8	0.115	0.1785	0.188
A13	89.6	0.525	0.1791	0.164
B11	75.8	0.22	0.2056	0.205
B12	82.7	0.58	0.2368	0.227
B13	89.6	1.01	0.2719	0.286
C11	75.8	0.87	0.4012	0.400
C13	89.6	1.76	0.8280	0.827

CHAPTER V

CONCLUSIONS

Creep tests of 6061-0 aluminum alloy had been conducted under different creep stresses and different constant strain rates at the loading stage. The endochronic theory of plasticity has been applied to described the experimental results.

Among the conclusions of this investigation are the following:

- Constant plastic-strain-rate tension tests are practical using a computer controlled test system.
- The plastic-strain-rate prior to creep has noticeable effect on creep behavior of metals.
- A nonlinear intrinsic time scale function has been proposed which will achieve a steady state at large intrinsic time.
- The strain-rate sensitivity function has been proposed as an archyperbolic sine function for 6061-0 aluminum alloy. The theory compares reasonably well with the experimental results.
- An exponential expression of the β_c coefficient has been used in this investigation, and the agreement is good.

APPENDIX A

BRIEF SUMMARY OF THE ENDOCHRONIC THEORY OF VISCOPLASTICITY

The endochronic theory of viscoplasticity developed by Valanis [15] is based on the notion of intrinsic time and the thermodynamic theory of internal variables. Since most of the materials are, in general, strain history dependent, the intrinsic time has been defined such that

$$d\zeta^2 = P_{ijkl}\, d\varepsilon_{ij}\, d\varepsilon_{kl} \tag{A1}$$

where ε_{ij} is the strain tensor and P_{ijkl} is a positive definite material tensor. In addition, a time scale $z(\zeta)$ is introduced such that $dz/d\zeta>0$. This concept together with the thermodynamic theory of internal variables give following explicit constitutive equation for isotropic materials under small isothermal deformation:

$$\sigma_{ij}=\delta_{ij}\int_0^z \lambda(z-z')\frac{\partial \varepsilon}{\partial z}dz' + 2\int_0^z \mu(z-z')\frac{\partial e}{\partial z}dz' \tag{A2}$$

where σ_{ij} is the stress tensor, e_{ij} is the deviatoric part of ε_{ij}, δ_{ij} is the kronecker's delta; and $\lambda(z)$ and $\mu(z)$ are heredity functions.

This definition of intrinsic time has led to difficulties in cases where the history of deformation involves unloading. Valanis has since introduced a new concept of intrinsic time to overcome these difficulties. In the one-dimensional case the new intricsic time ζ is defined as

$$d\zeta = \left| d\varepsilon - k_1 \frac{d\sigma}{E} \right| \tag{A3}$$

where k_1 is a positive scale such that $0 \le k_1 \le 1$, and E_0 is the elastic modulus. When $k_1=0$ the original form of intrinsic time is recovered, but when $k_1=1$, $\theta=\varepsilon-\sigma/E_0$ is the plastic strain, and

$$d\zeta = |d\theta| \tag{A4}$$

With this new definition of intrinsic time the constitutive equation is given by

$$\sigma = E_0 \int_0^z \rho(z-z') \frac{d\theta}{dz} dz' \tag{A5}$$

where

$$E_0 \rho(z) = \frac{E_0}{a_0} \delta(z) + E_1 e^{-az} \tag{A6}$$

in which a_0, a, and E_1 are material parameters, $\delta(z)$ is the delta function, and z is related to ζ by

$$z = \frac{1}{\beta} \ln(1+\zeta\beta) \tag{A7}$$

The kernel function $\rho(z)$ is generally the sum of a delta function and a numbers of exponential terms. In equation (A6), only one exponential term is shown for simplicity.

The new form of the endochronic theory is a rate-independent theory and has recently been extended by Wu and Yip [11] to describe the strain rate and strain rate history effects on material behavior. In this connection, another intrinsic time was introduced by

$$d\zeta = k(\theta,\dot{\theta})|d\theta| \tag{A8}$$

where $\dot{\theta}$ is the plastic strain rate. This is the generalized version of the original intrinsic time for viscoplasticity proposed by Valanis [15,16] and is true for any deformation.

For simplicity, it is assumed that k is a function only of $\dot{\theta}$, i.e.

$$d\zeta = k(\dot{\theta})|d\theta| \tag{A9}$$

during loading at constant plastic strain rate.

With this definition, it was shown in [11] that the yield stress σ_y is related to the strain-rate by

$$\sigma = \frac{\sigma_y^{\dot{\theta}}}{k(\sigma)}\left(\frac{d\zeta}{dz}\right) \tag{A10}$$

where $\sigma_y^{\dot{\theta}}$ is the initial yield stress (proportional limit) at a reference strain-rate. Also, the constant-plastic-strain-rate stress-strain relation was obtained by integration of equation (A5) as

$$\sigma = (1+\beta_1\theta)+[\sigma_0-(\sigma_0-\sigma_y)(1+\beta_1\theta)^{-n}] \qquad (A11)$$

in which $\beta_1=k\beta=E_t/\sigma_0$, $n=1+\alpha/\beta$ and

σ_0 is the intercept of the asymptotic line of equation (A11) with the stress axis; E_t is the tangert modulus of the aforementioned asymptotic line.

REFERENCES

1. Andrade, E. N. The Flow in Metals Under Large Constant Stresses. Proceedings of the Royal Socity, London, Vol. 90, Serics A, 1914, pp. 329.

2. Norton, F. H. Creep of Steel at High Temperatures, McGraw-Hill, New York, 1929.

3. Garofalo, F. Fundamentals of Creep and Creep-Raputure in Metals, Macmillan, New York, 1965.

4. Rabotnov, Yu. N. Creep Problemss in Structural Members, North Holland, New York, 1969.

5. Gittus, J. H. Creep, Viscoelasticity, and Creep Fracture in Solids, Halsted Press, Wiley, 1975.

6. Conway, J. B. Numberical Methods for Creep and Rupture Analyses, Gordon and Breach, New York, 1967.

7. Rice, J. R. 'On the Structure of Stress-Strain Relations for Time-Dependent Plastic Deformation in Metals', Trans. ASME 37E, 1970. pp. 728-737.

8. Hart, E. W. 'Constitutive Equations for the Nonelastic Deformation of Metals', J. Engr. Materials and Technology, 1976. pp. 193-202.

9. Miller, A. 'An Inelastic Constitutive Model for Monotonic Cylic, and Creep Deformation', J. Engr. Materials and Technology, vol.98, No.2, Apr. 1976, pp.97-113.

10. Valanis K. C. and Wu, H. C. Strain Rate and History Effect on the Deformation of Metals -Final Report, Division of Materials Engineering, The University of Iowa, 1976. Report G378-DME-76-012.

11. Wu, H. C. and Yip, M. C. 'Strain Rate and Strain Rate History Effects on the Dynamic Behavior of Metallic Materials', International Journal of Solids and Structure, vol. 16, 1980. pp.515-536.

12. Cernocky E. F. and Krempl E. 'A Theory of Viscoplasticity based on Infinitesimal Total Strain', Department of Mechanical Engineering, Rensselaer Polytechnic Institute, Troy, Report No. RPI CS 78-3, 1978.

13. Valanis, K. C. and Lalwani, S. A. 'Thermodynamics of Internal Variables in the Context of Absolute Reaction Rate Theory and the Notion of Intrinsic Time', Division of Materials Engineering, The University of Iowa, Report G378/123-DME-76-005, 1976.

14. Wu, H. C. and Chen, L. 'Endochronic Theory of Transient Creep and Creep Recovery', Part I and II, Division of Materials Engineering, The University of Iowa, 1979.

15. Valanis K. C. 'A Theory of Viscoplsticity without a Yield Surface', Part I and Part II, Archives of Mechanics, Vol. 23, 1971, pp.517-551.

16. Valanis, K. C. 'On the Foundations of the Endochronic Theory of Plasticity', Archives of Mechanics, Vol. 27, 1975, p.857.

17. Valanis, K. C. 'Fundamental Consequencos of a New Intrinsic Time Measure - Plasticity as a Limit of the Endochronic Theory', Archives of Mechanics vol.32, 1980, p.171.